Kinetics of the Hydrogen Abstraction from Carbon-3 of 1-Butanol by Hydroperoxyl Radical: Multi-Structural Variational Transition State Calculations of a Reaction with 262 Conformat...

ARTICLE *in* JOURNAL OF PHYSICAL CHEMISTRY LETTERS · JANUARY 2012

Impact Factor: 7.46 · DOI: 10.1021/jz201546e

3 AUTHORS, INCLUDING:

Prasenjit Seal
University of Minnesota Twin Cities
30 PUBLICATIONS **256** CITATIONS
SEE PROFILE

Donald Truhlar
University of Minnesota Twin Cities
1,342 PUBLICATIONS **81,884** CITATIONS
SEE PROFILE

THE JOURNAL OF PHYSICAL CHEMISTRY Letters

Letter

pubs.acs.org/JPCL

Kinetics of the Hydrogen Abstraction from Carbon-3 of 1-Butanol by Hydroperoxyl Radical: Multi-Structural Variational Transition-State Calculations of a Reaction with 262 Conformations of the Transition State

Prasenjit Seal, Ewa Papajak, and Donald G. Truhlar*

Department of Chemistry and Supercomputing Institute, University of Minnesota, Minneapolis, Minnesota 55455-0431, United States

Supporting Information

ABSTRACT: We estimated rate constants for the hydrogen abstraction from carbon-3 of 1-butanol by hydroperoxyl radical, a critically important reaction in the combustion of biofuel. We employed the recently developed multi-structural variational transition-state theory (MS-VTST), which utilizes a multifaceted dividing surface that allows us to include the contributions of multiple structures for reacting species and transition states. First, multi-configurational Shepard interpolation—based on molecular-mechanics-guided interpolation of electronic-structure Hessian data obtained by the M08 HX/jun-cc-pVTZ electronic model chemistry—was used to obtain the portion of the potential energy surface needed for single-structure variational transition-state theory rate constants including multidimensional tunneling; then, the M08-HX/MG3S electronic model chemistry was used to calculate multi-structural torsional anharmonicity factors to complete the MS-VTST rate constant calculations. The lowest-energy structures of the transition state have strongly bent hydrogen bonds. Our results indicate that neglect of multi-structural anharmonicity would lead to errors of factors of 0.3, 46, and 171 at 200, 1000, and 2400 K for this reaction.

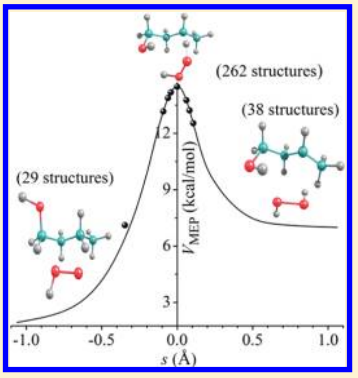

SECTION: Kinetics, Spectroscopy

Recent years have witnessed the emergence of 1-butanol as a promising candidate for new generation fuels.[1−13] Several features make 1-butanol a possible replacement of ethanol as a transport liquid fuel component; these include its high energy content, low vapor pressure, intoxicity to human health,[8,9] and decreased NO_x emission.[10] Wallner and coworkers[7] found that 1-butanol performs as well as ethanol in a direct-injection spark-ignition engine with an advantage of less fuel consumption; this further increases the interest in studying the combustion chemistry of 1-butanol in engines. Some recent research has also shown the potential of converting 1-butanol to alternative jet fuels.[12,13]

There have been several investigations of 1-butanol kinetics, both theoretical[1,4−6] and experimental.[2,3] Very recently, Karwat et al.[2] provided insight into the low-temperature combustion chemistry of 1-butanol by ignition and speciation studies. Previously, Vasu et al.[3] reported high-temperature rate constants of the ·OH radical with 1-butanol using shock tube and laser absorption. Simmie and coworkers[1] carried out theoretical work using VTST.

Hydrogen (H) abstraction by small radicals like ·OH, ·H, ·Cl, $\cdot CH_3$, and $\cdot O_2H$ plays an especially important role at high temperature. The $\cdot O_2H$ radical is an important species at intermediate temperatures in ignition, and its H abstraction reactions are an important source of H_2O_2, whose decomposition to form two ·OH radicals is also important. Therefore, the reaction of 1-butanol with $\cdot O_2H$ is important. The objective of the present Letter is to provide reliable theoretical rate constants for the H-atom abstraction from carbon-3 of 1-butanol by hydroperoxyl radical ($\cdot O_2H$) to yield 4-hydroxy-2-butyl radical and hydrogen peroxide

$$CH_3CH_2CH_2CH_2OH + \cdot O_2H \rightarrow CH_3C\cdot HCH_2CH_2OH + H_2O_2 \quad \text{(R1)}$$

Although there have been a number of studies of the abstraction of hydrogen atoms from 1-butanol by other radicals, particularly, ·OH,[1−4] we found only one result with $\cdot O_2H$. Black et al.[5] reported barrier heights for the site-specific abstraction of H atom from different sites of 1-butanol by $\cdot O_2H$.

Theory. The thermal rate constant is calculated by[14]

$$k^{\text{MS-CVT/SCT}} = F^{\text{MS-T}}(T)k^{\text{SS-CVT/SCT}}(T) \quad (1)$$

where $k^{\text{SS-CVT/SCT}}(T)$ and $k^{\text{MS-CVT/SCT}}(T)$ are the canonical variation theory (CVT) rate constants[15−17] in the single-structure[15−19] (SS) and multi-structural[14] (MS) approximations, respectively, employing multidimensional small-curvature tunneling (SCT),[20] and the factor $F^{\text{MS-T}}(T)$ accounts for the multiple-structure and torsional anharmonicity effects. Because $k^{\text{SS-CVT/SCT}}$ is based on scaled[21] frequencies, it includes some

Received: November 22, 2011
Accepted: January 3, 2012

   dx.doi.org/10.1021/jz201546e | J. Phys. Chem. Lett. 2012, 3, 264−271

nontorsional anharmonicity, but it does not include multi-structural anharmonicity due to multiple structures and torsions. We call $F^{\text{MS-T}}(T)$ the multi-structural torsional anharmonicity factor ratio, and it can be written in terms of multi-structural anharmonicity factors for reactant (R) and transition states (‡) as

$$F^{\text{MS-T}}(T) = \frac{F^{\ddagger}_{\text{MS-T}}}{F^{\text{R}}_{\text{MS-T}}} \tag{2}$$

The anharmonicity factors $F^{\chi}_{\text{MS-T}}$ of eq 2 can be factored as

$$F^{\chi}_{\text{MS-T}} = F^{\chi}_{\text{MS-LH}} F^{\chi}_{\text{T}} \tag{3}$$

where χ is R or ‡, MS-LH denotes the multiple-structure local harmonic approximation, and F^{χ}_{T} accounts for torsional anharmonicity. We calculate these factors as

$$F^{\chi}_{\text{MS-LH}} = \frac{Q^{\text{MS-LH}}_{\chi,\text{con-rovib}}(T)}{Q^{\text{SS-HO}}_{\chi,\text{rovib,GM}}(T)} \tag{4}$$

$$F^{\chi}_{\text{T}} = \frac{Q^{\text{MS-T}}_{\chi,\text{con-rovib}}(T)}{Q^{\text{MS-LH}}_{\chi,\text{con-rovib}}(T)} \tag{5}$$

where Q is the partition function for a given system, "con" denotes conformational, "rovib" denotes rotational–vibrational, GM denotes the global minimum geometry of a reagent or the transition state (TS, also denoted as ‡), and SS-HO denotes the single-structure harmonic oscillator approximation. We can rewrite eq 2 with the help of eqs 4 and 5 as

$$F^{\text{MS-T}}(T) = \frac{Q^{\text{MS-T}}_{\ddagger,\text{con-rovib}}(T)}{Q^{\text{MS-T}}_{\text{R,con-rovib}}(T)} \frac{Q^{\text{SS-HO}}_{\text{R,rovib,gm}}(T)}{Q^{\text{SS-HO}}_{\ddagger,\text{rovib,gm}}(T)} \tag{6}$$

In the present study, we followed a four-step procedure to obtain the MS-VTST thermal rate constants.

Structure Search. In the first step, we generated initial guesses of all structures of the reactant (1-butanol), products (4-hydroxy-2-butyl radical and hydrogen peroxide), and transition state (TS) by using a grid of initial torsional angles. Then, geometry optimizations were performed with the M08-HX[22]/MG3S[23] electronic model chemistry (chosen because of it good performance in previous validations[24−26]) using the ultrafine grid in the *Gaussian 09* program[27] with the *MN-GFM*.[28] Then, the unique optimized geometries were used for further optimization and vibrational frequency calculations with an integral grid of 99 radial shells and 974 angular points per shell.

The torsion angles that we used in searching for distinguishable structures are H5−O6−C1−C2, O6−C1−C2−C3, and C1−C2−C3−C4 for 1-butanol and 4-hydroxy-2-butyl radical and H10−O8−C1−C2, O8−C1−C2−C3, C1−C2−C3−C4, C2−C3−H17−O12, C3−H17−O12−O13, and H17−O12−O13−H14 for the TS. (See Figure 1.) When all torsions are independent and ideal, t three-fold torsions (excluding methyl groups) would generate 3^t structures. Because t is 3 for 1-butanol and 4-hydroxy-2-butyl radical and 6 for the TS, ideal torsions would generate 27 structures for 1-butanol and the product radical and 729 structures for the TS. However, the torsions are not ideal, and we found 29, 38 and 262 structures.

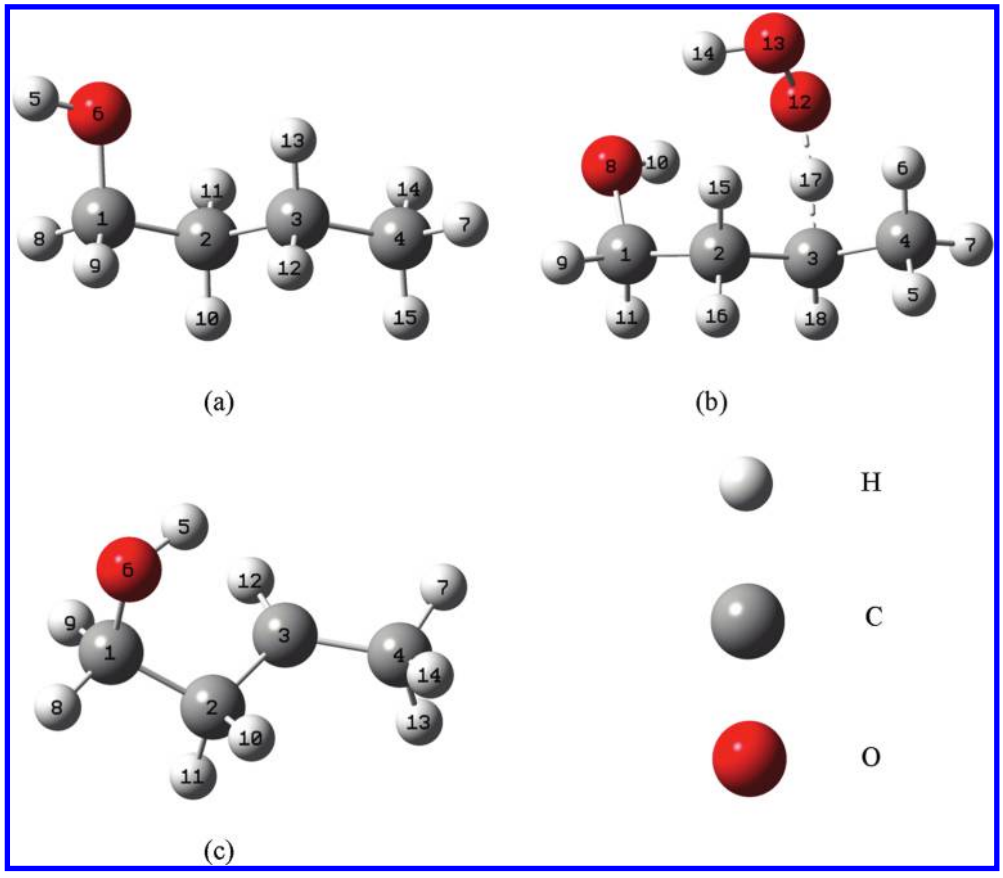

Figure 1. Global minimum structures of (a) 1-butanol, (b) transition state leading to the formation of 4-hydroxy-2-butyl radical, and (c) 4-hydroxy-2-butyl radical.

dx.doi.org/10.1021/jz201546e | *J. Phys. Chem. Lett.* 2012, 3, 264−271

The naming of the structures is based on the scheme previously presented.[29] For 1-butanol, the $\mathbf{T^-G^+T^-}$ conformer and its mirror image are the GM structures. The $\mathbf{G^+G^-T^+}$, $\mathbf{G^-G^+T^-}$ structures of 4-hydroxy-2-butyl radical have the lowest zero-point-exclusive and inclusive energies, and hence it is the GM structure of the product radical. For the TS, among 262 conformers, we found that the $\mathbf{G^+G^-T^+G^+C^+g^-}$ conformer and its mirror image have the lowest zero-point-inclusive and exclusive energies and is the GM structure. These GM structures are presented in Figure 1.

The relative conformational energies for each of the structures are given in Tables S1 and S2 of the Supporting Information. Although the relative conformational energies for 1-butanol and 4-hydroxy-2-butyl radical lie within a range of 2.25 kcal/mol, for the TS the range is 7.45 kcal/mol.

Multi-structural (MS) Partition Functions and Anharmonicity Factors (F). The second step is to determine Q and the F factors for the reactant, products, and TS; these were calculated with the Hessians from the formatted checkpoint files of the above optimizations by using the *MSTor* program.[30] The M08-HX/MG3S density functional frequencies are scaled by a standard scaling factor[21] of 0.973 to account for nontorsional anharmonicity and higher-order correlation effects. For 1-butanol, 4-hydroxy-2-butyl radical, and the TS, the Voronoi tessellation method[30,31] was used to calculate the local periodicity parameters, M_j,τ,[31] where j labels a structure and τ labels a torsional coordinate. We used 3D Voronoi calculations for 1-butanol and 4-hydroxy-2-butyl radical and 6D for transition state. The M_j,τ for 1-butanol, 4-hydroxy-2-butyl radical, and the TS are given in Tables S1 and S2 of the Supporting Information.

Validations of Density Functional Results. The third step consists of validating the density functionals to be used for the dynamics calculations. In the present study, we choose the combination of three Minnesota density functionals, that is, M06-2X,[32] M08-SO,[22] and M08-HX, and five basis sets, viz. MG3S[23] (same as 6-311+G(2df,2p)[33−35] basis for H, C and O), ma-TZVP,[36] maug-cc-pVTZ,[37] jun-cc-pVTZ,[38] and maug-cc-pVQZ.[37] The reason for choosing these methods is their good performance for reactive barrier heights.[24,25] We also performed coupled cluster (CCSD(T)-F12a)[39−41] single-point calculations with the *Molpro* program;[42] the combination of the extended basis set we used with the F12a method of including explicitly correlated double-excitation amplitudes should yield results close to the complete basis set limit much more efficiently than using popular extrapolation or scaling methods. Dual-level methods, also employing the efficient F12a scheme, have also been used where the corresponding energies are given by

$$E_{\text{jun-jun}} = E_{\text{CCSD(T)-F12a/jun-cc-pVDZ}} + (E_{\text{MP2-F12/jun-cc-pVTZ}} - E_{\text{MP2-F12/jun-cc-pVDZ}}) \quad (7)$$

$$E_{\text{jun-jun(HL)}} = E_{\text{CCSD(T)-F12a/jun-cc-pVTZ}} + (E_{\text{MP2-F12/jun-cc-pVQZ}} - E_{\text{MP2-F12/jun-cc-pVTZ}}) \quad (8)$$

These methods are called jun-jun and jun-jun(HL), respectively.

The mean unsigned error (MUE) is defined as the average of the absolute values of the errors of zero-point-exclusive forward ($V_f^{\ddagger}$) and reverse ($V_r^{\ddagger}$) barrier heights and energy of reaction, ΔU, where "error" is assessed relative to the benchmark jun-jun(HL) results at the same geometry. Table 1 gives the zero-point-exclusive barrier heights and reaction energies based on 19 electronic model chemistries. The Table shows that the smallest errors in $V_f^{\ddagger}$, $V_r^{\ddagger}$, and ΔU are given by the M08-HX/jun-cc-pVTZ, M08-HX/ma-TZVP, and M08-SO/maug-cc-pVQZ methods, respectively. The MUE is smallest (0.09 kcal/mol) for M08-HX/jun-cc-pVTZ, and hence we choose this method for dynamics calculations. For comparison to the single-point energies in Table 2, we note that the consistently optimized values of $V_f^{\ddagger}$, $V_r^{\ddagger}$, and ΔU with M08-HX/jun-cc-pVTZ are 14.50, 2.60, and 11.90 kcal/mol. The zero-point-inclusive forward and reverse barrier heights for M08-HX/jun-cc-pVTZ are found to be 12.89 and 2.16 kcal/mol.

Table 1. Forward and Reverse Classical Barrier Heights and Classical Energies of Reaction for the Hydrogen Abstraction from Carbon-3 of 1-Butanol (in kcal/mol)[a]

electronic model chemistry	$V_f^{\ddagger}$	$V_r^{\ddagger}$	ΔU	MUE[b]
M06-2X/MG3S	12.42	0.58	11.84	1.44
M08-HX/MG3S	14.04	1.85	12.18	0.59
M08-SO/MG3S	14.33	2.62	11.71	0.15
M06-2X/ma-TZVP	13.41	1.07	12.34	1.11
M08-HX/ma-TZVP	15.95	2.83	13.12	0.92
M08-SO/ma-TZVP	16.43	3.37	13.06	1.24
M06-2X/maug-cc-pVTZ	12.73	1.40	11.33	1.22
M08-HX/maug-cc-pVTZ	14.81	2.94	11.87	0.16
M08-SO/maug-cc-pVTZ	15.73	3.65	12.08	0.78
M06-2X/jun-cc-pVTZ	12.52	1.17	11.35	1.36
M08-HX/jun-cc-pVTZ	14.50	2.60	11.90	0.09
M08-SO/jun-cc-pVTZ	15.50	3.36	12.14	0.62
M06−2X/maug-cc-pVQZ	13.26	1.53	11.74	0.86
M08-HX/maug-cc-pVQZ	15.71	3.55	12.15	0.76
M08-SO/maug-cc-pVQZ	15.83	3.99	11.83	0.84
CCSD(T)-F12a/jun-cc-pVDZ	14.43	2.01	12.42	0.48
CCSD(T)-F12a/jun-cc-pVTZ	14.39	2.48	11.90	0.17
jun-jun	13.96	2.54	11.42	0.40
jun-jun(HL)	14.56	2.74	11.82	0.00

[a]To perform a consistent comparison, we calculated all results in this Table at the same set of three geometries, namely, those obtained by the M08-HX/MG3S method. In the context of the present table, "classical" means zero-point-exclusive. [b]Mean unsigned errors in the three energetic quantities are calculated with respect to the jun-jun (HL) method.

Recently, Simmie and coworkers[5] reported forward barrier heights for the abstraction of hydrogen atom from all possible sites of 1-butanol by $\cdot O_2H$ as calculated by several methods. Our computed results obtained with jun-jun (HL) method for the forward barrier height agree well with their G3 data,[5] but their B3LYP, M05-2X, MP2, and CBS-Q3 results underestimate the barrier heights.

Dynamics Calculations for the Rate Constant. In the final step, the electronic model chemistry with the smallest MUE was used to determine thermal rate coefficients via multiconfiguration Shepard interpolation (MCSI)[43−47] using single-structure (SS) VTST[15−17] with a curvilinear dividing surface[18,19] and a multidimensional small-curvature tunneling.[20] The MEP (V_{MEP}) and ground-state vibrationally adiabatic potential, V_a^G, were

dx.doi.org/10.1021/jz201546e | J. Phys. Chem. Lett. 2012, 3, 264−271

Table 2. Multi-Structural Torsional Anharmonicity Factors for the H-Abstraction from Carbon-3 of 1-Butanol by $\cdot O_2H$[a]

	multi-structural anharmonicity factors						
T (K)	$F^{R}_{MS\text{-}T}$	$F^{P1}_{MS\text{-}T}$	$F^{P2}_{MS\text{-}T}$	$F^{P}_{MS\text{-}T}$	$F^{\ddagger}_{MS\text{-}T}$	$F^{MS\text{-}T}_{forward}$	$F^{MS\text{-}T}_{reverse}$
200	9.72	13.60	2.00	27.20	3.45	0.35	0.13
250	12.10	19.00	2.00	38.00	5.16	0.43	0.14
298.15	14.30	23.90	2.00	47.80	8.69	0.61	0.18
300	14.40	24.00	2.00	48.00	8.88	0.62	0.19
400	18.40	32.00	2.00	64.00	31.60	1.72	0.49
500	21.70	36.90	2.00	73.80	95.20	4.39	1.29
600	24.20	39.60	2.00	79.20	220.0	9.09	2.78
800	27.00	40.20	2.00	80.40	662.0	24.52	8.23
1000	27.70	38.10	2.00	76.20	1260	45.49	16.53
1300	26.50	33.20	2.00	66.40	2120	80.00	31.93
1500	25.10	29.80	2.00	59.60	2550	101.59	42.79
1800	22.60	25.20	2.00	50.40	2940	130.09	58.33
2000	20.90	22.60	2.02	45.65	3060	146.41	67.03
2400	17.80	18.30	2.02	36.97	3040	170.79	82.23
3000	14.10	13.70	2.02	27.67	2700	191.49	97.58
4000	9.87	9.01	2.02	18.20	2000	202.63	109.89

[a] $F^{P}_{MS\text{-}T}$ in the table is the product of the F factors for the two products, 4-hydroxy-2-butyl radical (P1) and H_2O_2 (P2).

obtained with the MCSI[48] and MC-TINKERATE programs, and the rate constants were estimated using MC-TINKERATE[49] and POLYRATE[50,51] programs.

Results. The partition functions for the reacting species and TS were calculated in order to determine multi-structural anharmonicity factors (F). These F factors were then used to obtain forward and reverse MS-VTST rate constants for the reaction. These calculations use the MS-T multi-structural anharmonicity method to treat the torsions, including their coupling to other torsions and to overall rotation, thereby avoiding the assumption of independent torsions or limited torsional coupling. (It has been pointed out[52] that the independent-torsion approximation is particularly unreliable when some of the torsions can give rise to internal hydrogen bonding, as in the present system.) Table 2 provides the final $F_{MS\text{-}T}$ factors of 1-butanol, 4-hydroxy-2-butyl radical, H_2O_2, and the TS. The partition functions and other F factors for these systems are given in the Supporting Information. Table 2 shows where some $F_{MS\text{-}T}$ factors pass through a maximum. Maxima were also observed for F_T, whereas $F_{MS\text{-}LH}$ shows a gradual increase. (See Tables S4, S5, and S7 of the Supporting Information.) In Table 2, we also tabulated the ratio, $F^{MS\text{-}T}$, which is large and increases gradually.

For estimating the rate constants, we choose M08-HX/jun-cc-pVTZ frequencies and Hessians. The MCSI algorithm was used to find the minimum energy reaction path. Let s denote the reaction coordinate (s) scaled to a reduced mass of 1 amu. To obtain the potential energy surface in the vicinity of the minimum energy path, we follow same strategy as previously proposed.[44] The points in Figure 2a were taken at s = 0.0 Å (Point 1: saddle point geometry), s = −0.061 Å (Point 2: one-quarter down from the saddle point along the MCMM-0 reaction path on the dynamical bottleneck side), s = 0.061 Å (Point 3: one-quarter down from the saddle point along the MCMM-1 path on the side opposite to the dynamical bottleneck side), s = −0.092 Å (Point 4: one-half down from the saddle point along the MCMM-2 path on the dynamical bottleneck side), and so forth. The details of the total reaction path are given in the Supporting Information. This procedure results in a V_{MEP} profile that is well-converged. Figure 2a,b show V_{MEP} and V_a^G, respectively, as functions of s. The V_a^G profile is not well-converged in the foothills, but this has little effect on the combustion rate constants because the

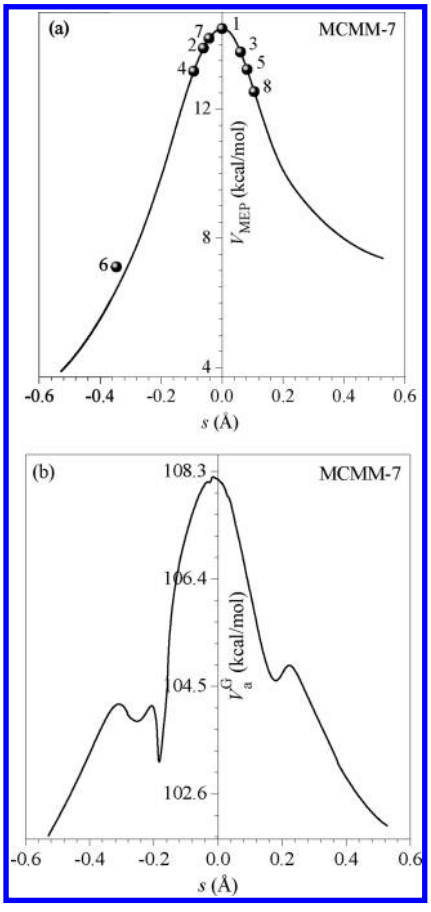

Figure 2. Estimated (a) V_{MEP} and (b) ground-state vibrationally adiabatic potential, V_a^G, plotted against the reaction coordinate, s, scaled to a reduced mass of 1 amu, for the H abstraction from carbon-3 of 1-butanol by $\cdot O_2H$ to form 4-hydroxy-2-butyl radical. Points 2−8 in Figure 2a are the nonstationary Shepard points that we consider to calculate the reaction path by following ref 44 Point 1 is the saddle point.

dx.doi.org/10.1021/jz201546e | J. Phys. Chem. Lett. 2012, 3, 264−271

Table 3. Forward and Reverse SS-VTST and MS-VTST Thermal Rate Constants (in cm^3 $molecule^{-1}$ s^{-1}) for the H-Abstraction from Carbon-3 of 1-Butanol by $\cdot O_2H$, the Activation Energy, E_a (in kcal/mol), of the Forward and Reverse Reaction, and the SCT Representative Tunneling Energy[a]

T (K)	forward rate coefficients		E_a for the forward reaction	reverse rate coefficients		E_a for the reverse reaction	SCT representative tunneling energy	T (K)
	$k^{SS\text{-}CVT/SCT}$	$k^{MS\text{-}CVT/SCT}$		$k^{SS\text{-}CVT/SCT}$	$k^{MS\text{-}CVT/SCT}$			
200	6.36×10^{-28}	2.26×10^{-28}	7.67	1.00×10^{-30}	1.27×10^{-31}	8.33	103.39	200
250	1.02×10^{-25}	4.35×10^{-26}	10.88	2.58×10^{-28}	3.50×10^{-29}	11.59	104.04	250
298.15	3.49×10^{-24}	2.12×10^{-24}	13.32	1.16×10^{-26}	2.11×10^{-27}	14.00	104.12	298.15
300	3.92×10^{-24}	2.42×10^{-24}	13.40	1.32×10^{-26}	2.44×10^{-27}	14.08	104.13	300
400	5.63×10^{-22}	9.67×10^{-22}	16.62	2.52×10^{-24}	1.24×10^{-24}	17.21	104.74	400
500	1.53×10^{-20}	6.71×10^{-20}	18.36	7.71×10^{-23}	9.95×10^{-23}	18.87	106.44	500
600	1.55×10^{-19}	1.41×10^{-18}	19.37	8.18×10^{-22}	2.27×10^{-21}	19.84	107.29	600
800	4.13×10^{-18}	1.01×10^{-16}	20.53	2.21×10^{-20}	1.82×10^{-19}	21.00	108.10	800
1000	3.69×10^{-17}	1.68×10^{-15}	21.33	1.95×10^{-19}	3.22×10^{-18}	21.84	108.13	1000
1300	3.24×10^{-16}	2.59×10^{-14}	22.43	1.66×10^{-18}	5.30×10^{-17}	23.04	108.15	1300
1500	9.62×10^{-16}	9.77×10^{-14}	23.19	4.85×10^{-18}	2.08×10^{-16}	23.87	108.17	1500
1800	3.43×10^{-15}	4.46×10^{-13}	24.40	1.70×10^{-17}	9.92×10^{-16}	25.19	108.19	1800
2000	6.21×10^{-15}	9.09×10^{-13}	25.23	3.04×10^{-17}	2.04×10^{-15}	26.10	108.19	2000
2400	7.64×10^{-15}	1.30×10^{-12}	26.98	3.69×10^{-17}	3.03×10^{-15}	28.00	108.20	2400
3000	2.32×10^{-14}	4.44×10^{-12}	29.71	1.11×10^{-16}	1.08×10^{-14}	30.96	108.20	3000
4000	8.53×10^{-14}	1.73×10^{-11}	34.45	4.03×10^{-16}	4.43×10^{-14}	36.09	108.20	4000

[a]Includes variational effects, torsional anharmonicity, and tunneling.

representative tunneling energies[53] (tabulated in Table 3) are above 104.7 kcal/mol for $T \geq 400$ K.

Table 3 and Figure 3 present the SS-VTST and MS-VTST forward and reverse rate constants. The figure illustrates that up

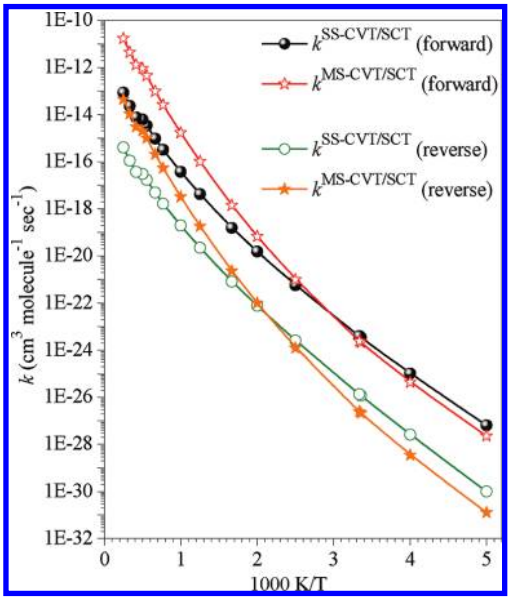

Figure 3. Calculated forward and reverse rate constants obtained by the MS-VTST method for the H-atom abstraction from carbon-3 of 1-butanol by $\cdot O_2H$ to form 4-hydroxy-2-butyl radical and hydrogen peroxide.

to 400 K, the SS-VTST and MS-VTST rate constants are within a factor of 3. Beyond 500 K, we obtain large deviations in rate constants, reaching a factor of 147 by 2000 K and then increasing further. This shows the importance of torsional factors at high temperatures. The MS-VTST rate constants fit well with the following physically motivated four-parameter expressions[54]

$$k_{R1}^{MS\text{-}CVT/SCT}(\text{forward}) = 1.53 \times 10^{-13}\left(\frac{T}{300}\right)^{2.56} \times \exp(-12.93(T + 197.18)/R(T^2 + 197.18^2)) \quad (9)$$

$$k_{R1}^{MS\text{-}CVT/SCT}(\text{reverse}) = 2.45 \times 10^{-16}\left(\frac{T}{300}\right)^{2.75} \times \exp(-13.08(T + 189.78)/R(T^2 + 189.78^2)) \quad (10)$$

where R is the gas constant, and the units are as in Table 3.

Table 3 also gives the activation energies, E_a, for the forward and reverse reaction in Table 3. The activation energies are calculated from eqs 9 and 10 and the definition

$$E_a = -R\frac{d(\ln k)}{d(1/T)} \quad (11)$$

The activation energies vary by 27.76 kcal/mol over the temperature range studied.

It is interesting to consider the presence of hydrogen bonding in the transition state because this has previously been observed for this[5] and similar[55] reactions. Various criteria have been used in the literature to classify whether an interaction should be called a hydrogen bond. For D−H···A interactions, where D is the donor atom and A is the acceptor atom, these criteria often involve the H···A distance, R(H···A), and the D−H···A bond angle, θ. The criteria depend on the atomic number and charge of D and A. After examining a number of hydrogen bonding studies, we decided to define a "normal" hydrogen bond by the criteria adopted by Chen et al.,[56] namely, for the case where both D and A are neutral oxygen, that R(H···A) ≤ 2.4 Å and $\theta \geq 150°$. Table S2 of the Supporting Information lists the 262 structures of the transition state (131 mirror image pairs) along with their structure numbers (in order of increasing energy) and their zero-point-exclusive and zero-point-inclusive energy values relative to the lowest-energy structure. For structures containing a normal hydrogen bond, there is an asterisk

dx.doi.org/10.1021/jz201546e | J. Phys. Chem. Lett. 2012, 3, 264−271

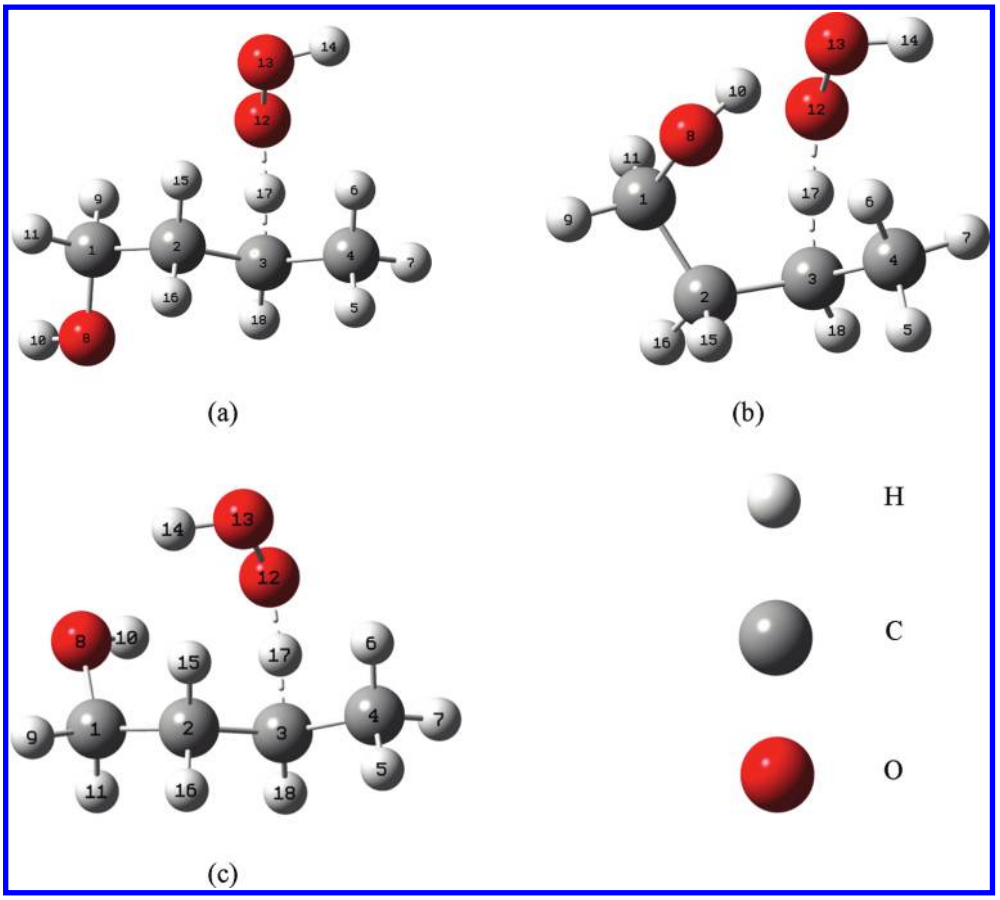

Figure 4. Lowest-energy TS structures with (a) no hydrogen bond, (b) a normal hydrogen bond, and (c) a strongly bent hydrogen bond.

after the pair of structure numbers. There is no universal agreement on the angle criterion, so we also identify another category of hydrogen bonds ("strongly bent hydrogen bonds"); these have $R(H\cdots A) \leq 2.4$ Å and $90 < \theta < 150°$. Strongly bent hydrogen bonds have two asterisks in Table S2 of the Supporting Information. Among 262 TS structures, 70 (including the 50 lowest-energy ones) have hydrogen bonds, of which 14 are normal and 56 are strongly bent. The lowest-energy structures with a normal hydrogen bond are the pairs 23, 24 and 27, 28 which respectively have H10···O13 and H10···O12 hydrogen bonds. Structures 1−16 have strongly bent H14····O8 hydrogen bonds, and structures 1−4 also have strongly bent H10···O12 hydrogen bonds. Further details are in Table S3 of the Supporting Information, and illustrative structures are in Figure 4.

Summary. We estimated the thermal rate constants for hydrogen abstraction from carbon-3 of 1-butanol by $\cdot O_2H$ by employing the recently developed MS-VTST method[14] for the temperature range 200−4000 K. The MS-VTST approach is a convenient way to include contributions of more than one structure for reagents and transition states, thereby yielding rate constants for complex reactions with multiple torsions. We applied the MCSI method[43−47] to obtain the portion of the potential energy surface needed to calculate the variational effect and tunneling contributions. To the best of our knowledge, there are no experimental and theoretical rate constant data for this reaction. Our results indicate that torsional factors are very important at higher temperatures, and neglecting these factors would lead to an error of a factor as large of 171 at 2400 K.

■ ASSOCIATED CONTENT

Supporting Information

Optimized Cartesian coordinates of the six lowest-energy structures of 1-butanol, 4-hydroxy-2-butyl radical, and the transition states and of hydroperoxyl radical and hydrogen peroxide; relative conformational energies and local periodicities; H-bonded TS structures and the relevant bond distances and angles; conformational-rotational−vibrational partition functions and anharmonicity factors; and details of the reaction path. This material is available free of charge via the Internet at http://pubs.acs.org.

■ AUTHOR INFORMATION

Corresponding Author

*E-mail: truhlar@umn.edu.

■ ACKNOWLEDGMENTS

We are grateful to Dr. Osanna Tishchenko and Dr. Jingjing Zheng for valuable contributions to the work. This work was partially supported by the U.S. Department of Energy, Office of Science, Office of Basic Energy Science, as part of the Combustion Energy Frontier Research Center under award number DE-SC0001198. Some of the computations were performed as part of a Computational Grand Challenge grant at the Molecular Science Computing Facility in the William R. Wiley Environmental Molecular Sciences Laboratory, a national scientific user facility sponsored by the U.S. Department of Energy's Office of Biological and Environmental Research and

located at the Pacific Northwest National Laboratory, operated for the Department of Energy by Battelle.

REFERENCES

(1) Zhou, C.-W.; Simmie, J. M.; Curran, H. J. Rate Constants for Hydrogen-Abstraction by ȮH from *n*-Butanol. *Combust. Flame* **2011**, *158*, 726−731.

(2) Karwat, D. M. A.; Wagnon, S. W.; Teini, P. D.; Wooldridge, M. S. On the Chemical Kinetics of *n*-Butanol: Ignition and Speciation Studies. *J. Phys. Chem. A* **2011**, *115*, 4909−4921.

(3) Vasu, S. S.; Davidson, D. F.; Hanson, R. K.; Golden, D. M. Measurements of the Reaction of OH with *n*-Butanol at High-Temperatures. *Chem. Phys. Lett.* **2010**, *497*, 26−29.

(4) Moc, J.; Simmie, J. M. Hydrogen Abstraction from *n*-Butanol by the Hydroxyl Radical: High Level Ab Initio Study of the Relative Significance of Various Abstraction Channels and the Role of Weakly Bound Intermediates. *J. Phys. Chem. A* **2010**, *114*, 5558−5564.

(5) Black, G.; Simmie, J. M. Barrier Heights for H-Atom Abstraction by $H\dot{O}_2$ from *n*-Butanol−A Simple Yet Exacting Test for Model Chemistries? *J. Comput. Chem.* **2010**, *31*, 1236−1248.

(6) Moc, J.; Simmie, J. M.; Curran, H. J. The Elimination of Water from a Conformationally Complex Alcohol: A Computational Study of the Gas Phase Dehydration of *n*-Butanol. *J. Mol. Struct.* **2009**, *928*, 149−157.

(7) Wallner, T.; Miers, S. A.; McConnell, S. A Comparison of Ethanol and Butanol as Oxygenates Using a Direct-Injection, Spark-Ignition (DISI) Engine. Proceedings of ASME 2008 Internal Combustion Engine Division Spring Technical Conference, Chicago, Illinois, April 28−30, 2008; ICES2008-1690.

(8) Jacobson, M. Z. Effects of Ethanol (E85) Versus Gasoline Vehicles on Cancer and Mortality in the United States. *Environ. Sci. Technol.* **2007**, *41*, 4150−4157.

(9) Fargione, J.; Hill, J.; Tilman, D.; Polasky, S.; Hawthorne, P. Land Clearing and the Biofuel Carbon Debt. *Science* **2008**, *319*, 1235−1238.

(10) Golombok, M.; Tierney, S. Effect of Oxygenates on Water Uptake in Hydrocarbon Fuels. *Ind. Eng. Chem. Res.* **1997**, *36*, 5023−5027.

(11) Westbrook, C. K. Chemical Kinetics of Hydrocarbon Ignition in Practical Combustion Systems. *Proc. Combust. Inst.* **2000**, *28*, 1563−1577.

(12) Wright, M. E.; Harvey, B. G.; Quintana, R. L. Highly Efficient Zirconium-Catalyzed Batch Conversion of 1-Butene: A New Route to Jet Fuels. *Energy Fuels* **2008**, *22*, 3299−3302.

(13) Harvey, B. G.; Quintana, R. L. Synthesis of Renewable Jet and Diesel Fuels from 2-Ethyl-1-hexene. *Energy Environ. Sci.* **2010**, *3*, 352−357.

(14) Yu, T.; Zheng, J.; Truhlar, D. G. Multi-Structural Variational Transition State Theory: Kinetics of the 1,4-Hydrogen Shift Isomerization of the Pentyl Radical with Torsional Anharmonicty. *Chem. Sci.* **2011**, *2*, 2199−2213.

(15) Garrett, B. C.; Truhlar, D. G. Criterion of Minimum State Density in the Transition State Theory of Bimolecular Reactions. *J. Chem. Phys.* **1979**, *70*, 1593−1598.

(16) Truhlar, D. G.; Garrett, B. C. Variational Transition-State Theory. *Acc. Chem. Res.* **1980**, *13*, 440−448.

(17) Truhlar, D. G.; Isaacson, A. D.; Garrett, B. C. *Theory of Chemical Reaction Dynamics*; Baer, M., Ed.; CRC Press: Boca Raton, FL, 1985; Vol. *4*, pp 65−137.

(18) Jackels, C. F.; Gu, Z.; Truhlar, D. G. Reaction-Path Potential and Vibrational Frequencies in Terms of Curvilinear Internal Coordinates. *J. Chem. Phys.* **1995**, *102*, 3188−3201.

(19) Fernandez-Ramos, A.; Ellingson, B. A.; Garrett, B. C.; Truhlar, D. G. Variational Transition State Theory with Multidimensional Tunneling. In *Reviews in Computational Chemistry*; Lipkowitz, K. B., Cundari, T. R., Eds.; Wiley-VCH: Hoboken, NJ, 2007; Vol. *23*, pp 125−232.

(20) Liu, Y.-P.; Lynch, G. C.; Truong, T. N.; Lu, D.-h.; Truhlar, D. G. Molecular Modeling of the Kinetic Isotope Effect for the [1,5]-Sigmatropic Rearrangement of *cis*-1,3-Pentadiene. *J. Am. Chem. Soc.* **1993**, *115*, 2408−2415.

(21) Alecu, I. M.; Zheng, J.; Zhao, Y.; Truhlar, D. G. Computational Thermochemistry: Scale Factor Databases and Scale Factors for Vibrational Frequencies Obtained from Electronic Model Chemistries. *J. Chem. Theory Comput.* **2010**, *6*, 2872−2887.

(22) Zhao, Y.; Truhlar, D. G. Exploring the Limit of Accuracy of the Global Hybrid Density Functional for Main-Group Thermochemistry, Kinetics, and Noncovalent Interactions. *J. Chem. Theory Comput.* **2008**, *4*, 1849−1868.

(23) Lynch, B. J.; Zhao, Y.; Truhlar, D. G. Effectiveness of Diffuse Basis Functions for Calculating Relative Energies by Density Functional Theory. *J. Phys. Chem. A* **2003**, *107*, 1384−1388.

(24) Zheng, J.; Zhao, Y.; Truhlar, D. G. The DBH24/08 Database and Its Use to Assess Electronic Structure Model Chemistries for Chemical Reaction Barrier Heights. *J. Chem. Theory Comput.* **2009**, *5*, 808−821.

(25) Alecu, I. M.; Zheng, J.; Zhao, Y.; Truhlar, D. G. Computational Study of the Reactions of Methanol with the Hydroperoxyl and Methyl Radicals. Part I: Accurate Thermochemistry and Barrier Heights. *J. Phys. Chem. A* **2011**, *115*, 2811−2829.

(26) Xu, X.; Alecu, I. M.; Truhlar, D. G. How Well Can Modern Density Functionals Predict Intermolecular Distances at Transition State. *J. Chem. Theory Comput.* **2011**, *7*, 1667−1676.

(27) Frisch, M. J.; Trucks, G. W.; Schlegel, H. B.; Scuseria, G. E.; Robb, M. A.; Cheeseman, J. R.; Scalmani, G.; Barone, V.; Mennucci, B.; Petersson, G. A.et al. *Gaussian 09*, revision A.1; Gaussian, Inc.: Wallingford, CT, 2009.

(28) Zhao, Y.; Peverati, R.; Yang, K.; Truhlar, D. G. *MN-GFM*, version 5.2 computer program module; University of Minnesota, Minneapolis, MN, 2011.

(29) Seal, P.; Papajak, E.; Yu, T.; Truhlar, D. G. Statistical Thermodynamics of 1-Butanol, 2-Methyl-1-Propanol, and Butanal. *J Chem. Phys.* **2012**, in press.

(30) Zheng, J.; Mielke, S. L.; Clarkson, K. L.; Truhlar, D. G. *MSTor computer program*, version 2011; University of Minnesota: Minneapolis, MN, 2011.

(31) Zheng, J.; Yu, T.; Papajak, E.; Alecu, I. M.; Mielke, S. L.; Truhlar, D. G. Practical Methods for Including Torsional Anharmonicity in Thermochemical Calculations on Complex Molecules: The Internal-Coordinate Multi-Structural Approximation. *Phys. Chem. Chem. Phys.* **2011**, *13*, 10885−10907.

(32) Zhao, Y.; Truhlar, D. G. The M06 Suite of Density Functionals for Main Group Thermochemistry, Kinetics, Noncovalent Interactions, Excited States, and Transition Elements: Two New Functionals and Systematic Testing of Four M06 Functionals and Twelve Other Functionals. *Theor. Chem. Acc.* **2008**, *120*, 215−241.

(33) Krishnan, R.; Binkley, J. S.; Seeger, R.; Pople, J. A. Self-Consistent Molecular Orbital Methods. XX. A Basis Set for Correlated Wave Functions. *J. Chem. Phys.* **1980**, *72*, 650−654.

(34) Clark, T.; Chandrasekhar, J.; Spitznagel, G. W.; Schleyer, P. v. R. Efficient Diffuse Function-Augmented Basis Sets for Anion Calculations. III. The 3-21+G Basis Set for First-Row Elements, Li−F. *J. Comput. Chem.* **1983**, *4*, 294−301.

(35) Frisch, M. J.; Pople, J. A.; Binkley, J. S. Self-Consistent Molecular Orbital Methods 25. Supplementary Functions for Gaussian Basis Sets. *J. Chem. Phys.* **1984**, *80*, 3265−3269.

(36) Zheng, J.; Xu, X.; Truhlar, D. G. Minimally Augmented Karlsruhe Basis Sets. *Theor. Chem. Acc.* **2011**, *128*, 295−305.

(37) Papajak, E.; Truhlar, D. G. Efficient Diffuse Basis Sets for Density Functional Theory. *J. Chem. Theory Comput.* **2010**, *6*, 597−601.

(38) Papajak, E.; Truhlar, D. G. Convergent Partially Augmented Bases for Post-Hartree-Fock Calculations of Molecular Properties and Reaction Barrier Heights. *J. Chem. Theory Comput.* **2011**, *7*, 10−18.

(39) Adler, T. B.; Knizia, G.; Werner, H.-J. A. Simple and Efficient CCSD(T)-F12 Approximation. *J. Chem. Phys.* **2007**, *127*, 221106−221109.

(40) Knizia, G.; Adler, T. B.; Werner, H.-J. Simplified CCSD(T)-F12 Methods: Theory and Benchmarks. *J. Chem. Phys.* **2009**, *130*, 054104−054123.
(41) Manby, F. R. Density Fitting in Second-Order Linear-r_{12} Møller−Plesset Perturbation Theory. *J. Chem. Phys.* **2003**, *119*, 4607−4613.
(42) Werner, H.-J.; Knowles, P. J.; Manby, F. R.; Schütz, M.; Celani, P.; Knizia, G.; Korona, T.; Lindh, R.; Mitrushenkov, A.; Rauhut, G.et al. *Molpro*, version 2010.1; University of Birmingham: Birmingham, AL, 2010.
(43) Kim, Y.; Corchado, J. C.; Villa, J.; Xing, J.; Truhlar, D. G. Multiconfiguration Molecular Mechanics Algorithm for Potential Energy Surfaces of Chemical Reactions. *J. Chem. Phys.* **2000**, *112*, 2718−2735.
(44) Albu, T. V.; Corchado, J. C.; Truhlar, D. G. Molecular Mechanics for Chemical Reactions: A Standard Strategy for Using Multiconfiguration Molecular Mechanics for Variational Transition State Theory with Optimized Multidimensional Tunneling. *J. Phys. Chem. A* **2001**, *105*, 8465−8487.
(45) Lin, H.; Zhao, Y.; Tishchenko, O.; Truhlar, D. G. Multi-Configuration Molecular Mechanics Based on Combined Quantum Mechanical and Molecular Mechanical Calculations. *J. Chem. Theory Comput.* **2006**, *2*, 1237−1254.
(46) Tischenko, O.; Truhlar, D. G. Optimizing the Performance of the Multiconfiguration Molecular Mechanics Method. *J. Phys. Chem. A* **2006**, *110*, 13530−13536.
(47) Tischenko, O.; Truhlar, D. G. Non-Hermitian Multiconfiguration Molecular Mechanics. *J. Chem. Theory Comput.* **2009**, *5*, 1454−1461.
(48) Tishchenko, O.; Higashi, M.; Albu, T. V.; Corchado, J. C.; Kim, Y.; Villà, J.; Xing, J.; Lin, H.; Truhlar, D. G. *MCSI*, version 2010; University of Minnesota: Minneapolis, MN, 2010.
(49) Albu, T. V.; Tishchenko, O.; Corchado, J. C.; Kim, Y.; Villà, J.; Xing, J.; Lin, H.; Higashi, M.; Truhlar, D. G. *MC-TINKERATE*, version 2010; University of Minnesota: Minneapolis, MN, 2010.
(50) Zheng, J.; Zhang, S.; Lynch, B. J.; Corchado, J. C.; Chuang, Y.-Y.; Fast, P. L.; Hu, W.-P.; Liu, Y.-P.; Lynch, G. C.; Nguyen, K. A.et al. *POLYRATE*, version 2010-A; University of Minnesota: Minneapolis, MN, 2010.
(51) Lu, D.-h.; Truong, T. N.; Melissas, V.; Lynch, G. C.; Liu, Y.-P.; Garrett, B. C.; Steckler, R.; Isaacson, A. D.; Rai, S. N.; Hancock, G. C.; et al. POLYRATE 4: A New Version of a Computer Program for the Calculation of Chemical Reaction Rates for Polyatomics. *Comput. Phys. Commun.* **1992**, *71*, 235−262.
(52) Sharma, S.; Raman, S.; Green, W. H. Intramolecular Hydrogen Migration in Alkylperoxy and Hydroperoxyalkylperoxy Radicals: Accurate Treatment of Hindered Rotors. *J. Phys. Chem. A* **2010**, *114*, 5689−5701.
(53) Garrett, B. C.; Truhlar, D. G. Critical Tests of Variational Transition State Theory and Semiclassical Tunneling Methods for Hydrogen and Deuterium Atom Transfer Reactions and Use of the Semiclassical Calculations to Interpret the Overbarrier and Tunneling Dynamics. *J. Phys. Chem.* **1991**, *95*, 10374−10379.
(54) Zheng, J.; Truhlar, D. G. Kinetics of Hydrogen-Transfer Isomerizations of Butoxyl Radicals. *Phys. Chem. Chem. Phys.* **2010**, *12*, 7782−7793.
(55) Tishchenko, O.; Ilieva, S.; Truhlar, D. G. Communication: Energetics of Reaction Pathways for Reactions of Ethenol with the Hydroxyl Radical: The Importance of Internal Hydrogen Bonding at the Transition State. *J. Chem. Phys.* **2010**, *133*, 021102.
(56) Chen, C.; Li, W. Z.; Song, Y. C.; Yang, J. Hydrogen Bonding Analysis of Glycerol Aqueous Solutions: A Molecular Dynamics Simulation Study. *J. Mol. Liq.* **2009**, *146*, 23−28.